

Slip behavior during pressure driven flow of Laponite suspension

Propesar M. Kamdi,^{1,2} Ashish V. Orpe,^{1,2, a)} and Guruswamy Kumaraswamy^{1, b)}

¹⁾ *CSIR-National Chemical Laboratory, Pune 411008 India*

²⁾ *Academy of Scientific and Innovative Research (AcSIR), Ghaziabad 201002 India*

We investigate pressure driven pipe flow of Laponite suspension, as a model thixotropic fluid. The tendency of the suspension to age is controlled by addition of sodium chloride salt to vary the ionic strength. We use a syringe pump to prescribe the flow and observe that a steady state flow is obtained. Unusually, the steady state pressure drop required to maintain a constant flow rate decreases with increase in flow rate, in qualitative contrast to the expectation for Poiseuille flow. We demonstrate that experimental results obtained by varying the flow rate, salt concentration and flow geometry (pipe diameter and length) can be collapsed onto a single universal curve, that can be rationalized by invoking slip of the suspension at the tube walls. The Laponite suspension exhibits plug-like flow, yielding at the tube walls. Our results suggest that the slip length varies linearly with the flow rate and inversely with the tube diameter.

I. INTRODUCTION

The no-slip boundary condition is commonly invoked at liquid-solid interfaces. This dictates that the liquid velocity at the interface is equal to that of the solid. However, depending on the characteristics of the liquid or that of the wall, liquids can slip at the interface. For Newtonian liquids, slip has mostly been attributed to non-wettability of the surface¹⁻⁵ with a shear dependent slip length obtained theoretically for laminar flows⁶. For a laminar flow flow through a pipe, slip results in a distinct deviation from Poiseuille flow and, can get further exaggerated with decrease in system size⁷. An elegant theoretical treatment by Lauga and Stone⁸ accounts for slip during pressure driven flow through a capillary in terms of an effective slip length that depends on system and material properties. Others have applied a similar methodology to investigate the slip during flow of visco-plastic fluids in various geometries, and have demonstrated a scaling law for the slip velocity expressed in terms of wall shear stress and slip length^{9,10}. The predictions of the velocity profiles incorporating the scaling law, were shown to agree well with experimental measurements¹¹. In a later experimental study, it was shown that the scaling law holds only when the material has yielded across the entire flowing cross-section but not for co-existing solid-liquid regions or flows below the yield threshold¹². For shear-thinning visco-plastic fluids, wall slip in the regime beyond yielding, was shown to be enhanced compared to that for Newtonian liquids, while the opposite was observed for shear-thickening fluids¹³.

A common feature running across all the studies described above is the time independent nature of the fluid response. However, fluids that exhibit time dependent or thixotropic behavior are not uncommon. For example, crude oil that is pumped over large distances in pipelines comprises a thixotropic paraffin gel¹⁴. In the human body, biliary sludge comprising bacteria and particulates flows through viscoelastic gastrointestinal channels or through artificial stents^{15,16}. The effect of slip on pressure driven flow of thixotropic fluids remains poorly understood¹⁷ which makes it that much difficult to recover simple scaling laws characterising the slip behavior. A recent theoretical work showed that while the steady state flow

^{a)}Electronic mail: av.orpe@ncl.res.in

^{b)}Currently at Indian Institute of Technology Bombay, Powai, Mumbai 400076 India; Electronic mail: guruswamy@iitb.ac.in

condition for a thixotropic fluid is uniquely determined by the applied stress, the evolution to steady state is determined by the build up and breakage of the fluid microstructure¹⁸.

Here, we experimentally study the pressure driven flow of a model thixotropic fluid through a cylindrical tube to investigate the influence of slip on overall flow. We employ aqueous suspensions of an inorganic synthetic clay, Laponite, as a model thixotropic fluid, whose time dependent response can be controlled by addition of salt. Laponite comprises disk-shaped particles of ≈ 25 nm diameter and 0.92 nm thickness. When Laponite is vigorously stirred into water, clay platelets disperse to form a clear suspension. On ageing, platelet-platelet interactions result in the formation of larger scale microstructure in the dispersion such that it becomes increasingly viscous. At moderate concentrations, of the order of a few percent (by weight), aqueous Laponite dispersions develop a yield stress and exhibit solid-like response. Addition of sodium chloride salt to the aqueous dispersion modifies platelet-platelet electrostatic interactions such that the ageing process is significantly accelerated. Time dependent structure formation and relaxation phenomena in Laponite have been extensively researched in the last few decades^{19–25}. Researchers have reported a state diagram that describes the non-equilibrium structure formation in Laponite as a function of clay concentration and ionic strength²³. The precise physical mechanism for self-assembly in Laponite dispersions remains contentious, with arguments for both gel^{19,20,26–28} and glass^{29–36} formation. Our work does not address the question of the underlying structure that determines the rheology of Laponite dispersions. Of interest to us is only that Laponite self assembles in water to form a thixotropic dispersion, and that the paste-like rheology of Laponite dispersions is strongly influenced by the addition of sodium chloride salt.

II. EXPERIMENTAL DETAILS

A. Materials

Laponite was obtained from BYK additives Ltd. UK, and was used as received. Sodium chloride was obtained from Merck Specialities Pvt. Ltd. Mumbai and was used as received. Distilled deionized water (conductivity = $18 \mu\text{S}/\text{cm}$) was obtained from Millipore system (Merck Specialities Pvt. Ltd, Mumbai) and was used immediately.

B. Methods

We measured the pressure drop required to flow aqueous Laponite dispersion at a constant flow rate through a tube of length, L , and diameter, D , as shown in fig. 1. Dry Laponite powder and deionized water (Millipore) were continuously added to a vessel and were subjected to high speed shearing (Ultraturrax homogenizer, IKA). The vessel was kept immersed in a water bath to maintain the temperature of Laponite-water mixture at 25°C throughout the experiments. The outflow rate (q_1) from the vessel, as set by the peristaltic pump was the same as the inlet flow rate to the vessel which was set by the syringe pump. This ensured that volume of suspension (V) in the vessel is maintained constant throughout. The average residence time of the material in the mixer is maintained at 45 min. The high shear mixing protocol ensured that the state of the Laponite dispersion remained constant throughout the duration of the experiment. This was verified by measuring the outflow mass flow rate from the vessel which remained constant in time. To damp out fluctuations due to the peristaltic pump, the suspension is passed through a dampener (see section I in supplementary material). Downstream of the dampener, we introduce a second stream (volumetric flow rate, $q_2 = 0.13q_1$) using a needle and mix these streams by passing them through a pinched tube static mixer (see section II in supplementary material). The syringe pump that injects the second stream has two barrels so that it can flow either deionized water, or a salt (NaCl) solution for a fixed duration. After mixing in the static mixer, the

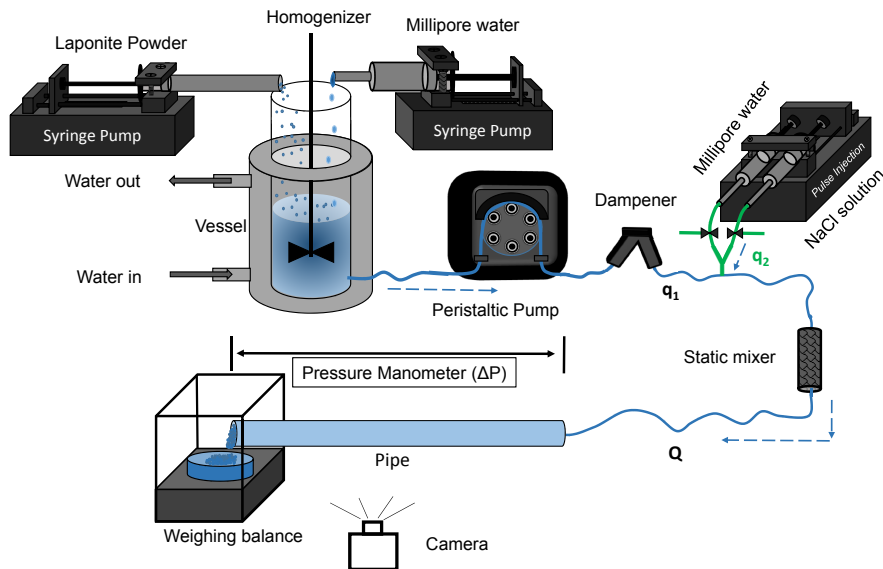


FIG. 1. Schematic of the experimental assembly showing continuous preparation and pumping of Laponite suspension through a tube. The assembly allows addition of salt (NaCl) solution in fixed quantities and for a fixed duration.

suspension is passed through the tube. The tube entrance has a uniformly diverging taper to minimize entrance effects due to change in cross-sectional area when the flow enters the tube. The tube exit is open to atmosphere and we use a pressure gauge just before the tube entrance to measure the pressure drop across the tube length. The total volumetric flow rate ($Q = q_1 + q_2$) in the system is set by the peristaltic and syringe pumps. The measured outflow mass flow rate from the tube remained constant in time. Experiments are performed for three flow rates ($Q = 0.46, 0.69$ and $0.92 \text{ cm}^3/\text{min}$) and at three salt concentrations (6, 9 and 12 mM, after the two streams are mixed). Tubes with different dimensions were used in the experiments: Glass tube (lengths 15.5 and 30 cm each with an internal diameter of 0.4 cm and 0.72 cm) and steel tube (length 23 and 53 cm each with an internal diameter of 0.1 cm). The Laponite concentration in all experiments was kept unchanged throughout at 3.1 wt %.

C. Pressure drop measurements

The time variation of the measured pressure difference (ΔP) across the cylindrical tube during the flow of Laponite suspension (with or without added salt), is shown in fig. 2 for a fixed tube diameter, fixed salt concentration and fixed flow rate. The variation of pressure difference for the Laponite suspension without salt is quite negligible and remains constant throughout at 0.06 kPa. We refer to this value as the base or reference pressure.

The addition of salt solution pulsed for $\Delta t_p = 80$ mins, however, increases the pressure difference significantly above the base value and achieves a near saturated state (with associated fluctuations). These are shown for three independent runs (red, green and blue solid lines in fig. 2). Presence of high salt concentration in Laponite suspension causes it to age rapidly with an evolving microstructure comprising sample spanning aggregates, thereby increasing the overall viscosity. This increase in the viscosity leads to increased pressure difference above the base value. The near saturated value of the pressure drop reflects a balance in the microstructure of the Laponite suspension, between the salt-induced ageing and flow effects. Following the stoppage of the salt solution pulse after Δt_p , the pressure difference returns to the base value over time suggesting that the salt has been removed

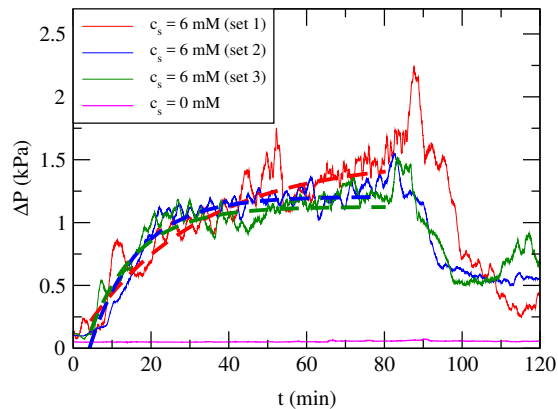


FIG. 2. Time (t) dependent pressure drop (ΔP) for the flow of Laponite suspension at a constant rate ($Q = 0.46 \text{ cm}^3/\text{min}$) through the tube of length ($L = 15.5 \text{ cm}$) and diameter ($D = 0.72 \text{ cm}$) for a fixed salt concentration ($C_s = 6 \text{ mM}$). Magenta colored solid line represents data without addition of salt, while three solid lines of different color (red, green and blue), respectively, represent three independent runs for addition of salt solution for a pulse of 80 minutes duration ($C_s = 6 \text{ mM}$). The dashed lines of red, green and blue color represent a fitted non-linear equation to the respective pressure data to extract the saturated value of pressure drop (ΔP_s). (see text for more details).

from the tube completely during that time. It can be noted that the timescales leading to the saturated value of pressure drop and while reverting to the base value are not the same. We believe that this difference owes its origin to (i) significant heterogeneity in the microstructures formed within the system and (ii) possibility of traces of microstructures remaining in the tube over much longer time duration while allowing for the flow of Laponite suspension (without salt) associated with pressure drop larger than the base value. Similar qualitative behavior for pressure drop variation is also observed for different tube diameters, lengths, salt concentration and flow rates investigated in this work.

The value of the plateau or the saturated pressure drop (ΔP_s) is extracted by fitting the data for the 80 minutes salt solution pulse with an exponential expression of the form $\Delta P = C_1(1 - \exp(-t/\tau)) + C_2$. The saturation value (ΔP_s) is then obtained as $C_1 + C_2$. The fit of this equation to the three independent runs is shown as dashed lines in red, green and blue colour in fig. 2. The parameters C_1 , C_2 and τ were simply used to fit the expression to the data and are observed to vary across three independent sets. We note similar time dependence for the pressure difference for all the flow rates, tube diameters and salt concentrations employed. For each case, 2 or 3 independent sets were performed and the data is reported for all the sets in subsequent figures.

III. RESULTS AND DISCUSSION

In Secs. IIIA and IIIB, we discuss the effect of tube length, flow rate, tube diameter and salt concentration on the observed variations in the saturated value of pressure drop (ΔP_s). We, then, try and show the scaling of all the data in Sec. IIIC based on simple flow modeling and heuristic arguments.

A. Effect of tube length and flow rate on saturated pressure drop

The variation of the saturated state pressure drop (ΔP_s) with flow rate (Q) for two different tube lengths, at fixed tube diameter ($D = 0.1 \text{ cm}$) and salt concentration ($c_s = 9$

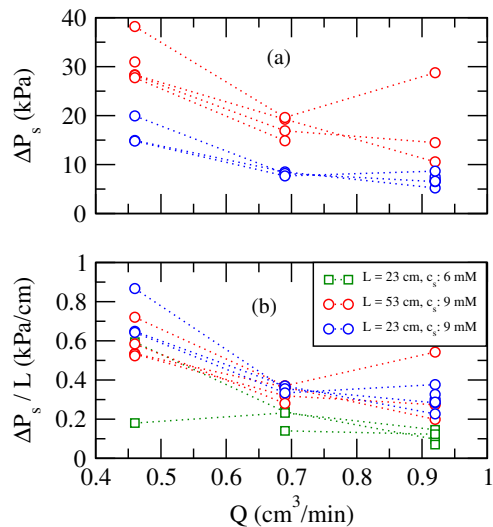


FIG. 3. Variation of (a) saturated pressure drop (ΔP_s) with flow rate in a tube of diameter ($D = 0.1$ cm) and salt concentration ($c_s = 9$ mM) for two different tube lengths and (b) Variation of $\Delta P_s/L$ with flow rate in a tube of diameter ($D = 0.1$ cm) and two salt concentrations and tube lengths.

mM) is shown in fig. 3a. For a given flow rate, the pressure drop increases with increase in the tube length. However, the pressure drop per unit length ($\Delta P_s/L$) is nearly independent of tube length as shown in fig. 3b. This suggests that the observed behavior and underlying mechanism is not localised, but it remains the same everywhere along the tube length.

Interestingly, the data in fig. 3b shows that the saturated pressure drops decreases monotonically with increase in the flow rate. Further, this decrease in the pressure drop is more prominent at higher salt concentration. At much higher salt concentration ($c_s = 12$ mM), rapid increase in viscosity led to intermittent flow causing problems in pressure drop measurements. This behavior of pressure drop is qualitatively opposite to that predicted by the Poiseuille equation. To rationalize this, we consider the possibility that higher shear rates at higher Q might result in a flow-induced breakdown of Laponite microstructure in the bulk of the suspension. This microstructural change correlates with a decrease in viscosity and therefore a decrease in $\Delta P_s/L$ with increase in Q . Such a behaviour, akin to a shear thinning fluid, will always yield an increase in the steady (or saturated) state pressure drop with increase in the flow rate in contrast to the observed behavior over here. Further, we anticipate that such flow-induced microstructural breakage will occur locally - thus, an increase in tube length should result in greater microstructural change and lower $\Delta P_s/L$. In this situation, $\Delta P_s/L$ will not be independent of the tube length, which is inconsistent with the behavior observed in fig. 3b. Therefore, the decrease in $\Delta P_s/L$ with Q is not a consequence of flow-induced changes in Laponite microstructure in the bulk of the tube. We now consider the possibility that slip of Laponite suspensions at the tube walls reduces the pressure drop. Similar behavior, i.e. increase in the flow rate under constant pressure gradient, been observed previously for pressure-driven flow of Newtonian liquids⁷ and visco-plastic fluids¹¹.

B. Effect of tube diameter and salt concentration on saturated pressure drop

Figure 4 shows the variation of $\Delta P_s/L$ with tube diameter for three different flow rates and three different salt concentrations. The values of $\Delta P_s/L$ decrease with increase in tube diameter at all flow rates and salt concentrations employed. This effect is more pronounced at smaller tube diameters. The inverse dependence is in line with the behavior expected

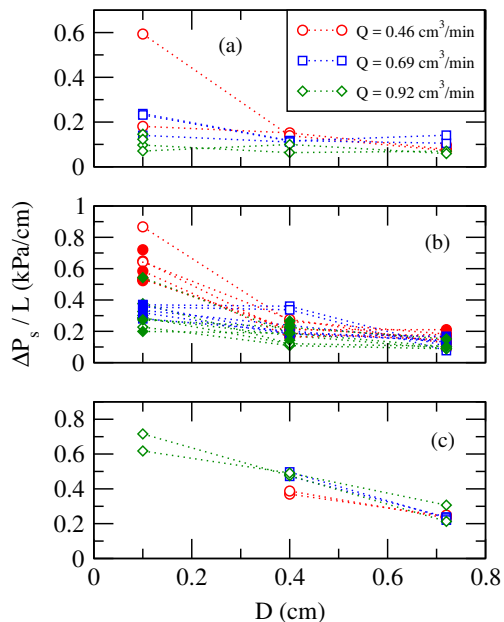


FIG. 4. (a) Variation of saturated pressure drop per unit length ($\Delta P_s/L$) with tube diameter (D) for three flow rates (Q). Panels (a), (b) and (c) represent, respectively, data obtained for salt concentrations, $c_s = 6$ mM, $c_s = 9$ mM and $c_s = 12$ mM. Open circles represent data for $L = 23$ cm, filled circles represent data for $L = 53$ cm, open squares and diamonds represent data for $L = 15.5$ cm and filled squares and diamonds represent data for $L = 30$ cm.

during the Poiseuille flow, i.e. smaller the cross-sectional area available for flow, higher is the pressure drop needed to achieve the same flow rate. Secondly, the magnitude of saturated pressure drop increases significantly with increase in salt concentration. Now, increase in salt concentration significantly accelerates ageing of Laponite suspensions, thereby increasing its effective viscosity²³. Naturally, the pressure drop required to pump the fluid at a constant rate is expected to increase with increase in the effective viscosity, in line with that expected from the Poiseuille flow. The effective viscosity rises rapidly with salt concentration, so that pressure drop measurements could be obtained only at the highest flow rate employed for experiments using the smallest tube diameter ($D = 0.1$ cm) at the highest salt concentration employed ($c_s = 12$ mM).

The parametric dependence described above shows distinct dependence of the measured pressure drop on three variables, namely flow rate, tube diameter and salt concentration. The salt content tends to influence the viscosity while the flow cross-section is governed by the tube diameter. However, both these effects seem to occur on the backdrop of flow slippage as evidenced by the observed dependence on employed flow rate. This encourages us to seek a non-linear dependence, akin to a scaling law relating these three variables with the saturated pressure drop. In the following we attempt to obtain a scaling relation from the experimental observations.

C. Scaling behavior

The Laponite suspension exhibits significant thixotropy, i.e. its state evolves continuously with waiting time. A steady state is, thus, not achievable in such a system, thereby precluding the existence of a stress constitutive equation comprising a steady shear viscosity. However, the experimental observations exhibit steady (or saturated) state pressure drop following initial transient period (see fig. 2). Given our primary interest in under-

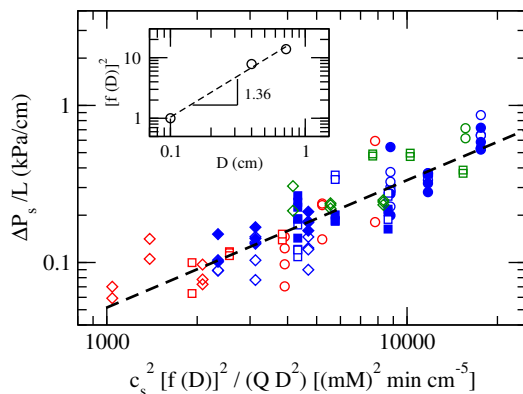


FIG. 5. Scaling of saturated pressure drop per unit length ($\Delta P_s/L$) with different experimental parameters investigated. Inset: Variation of shift factor $[f(D)]^2$ with tube diameter.

standing the behavior of steady pressure drop, we assume a unidirectional, steady state flow of Laponite suspension through the tube. Typically, a viscous laponite suspension exhibits a yield stress (τ_y) and a shear flow post yielding. To simplify the representation of the observed behavior, we consider Bingham fluid like behavior for which the shear stress is expressed as $\tau = \tau_y + \mu\dot{\gamma}$, where $\dot{\gamma}$ is the shear rate, μ is the shear viscosity. Using these assumptions and following the previous treatment for flow of Newtonian liquids⁸ and visco-plastic fluids⁹ through a cylindrical tube, the volumetric flow rate can be obtained as

$$Q = \frac{\pi D^4}{64} \left(\frac{\Delta P_s}{\mu L} \right) \left(1 - \lambda + \frac{2\delta}{D} \right)^2 \left[1 - 2 \left(\frac{(1-\lambda)^2}{4} + \frac{(1-\lambda)\lambda}{3} \right) \right] \quad (1)$$

where $\lambda = \tau_y/(\Delta P_s D/4L)$ and δ is the slip length. The overall form of the Eq. ?? is consistent with that obtained previously for a visco-plastic fluid⁹.

The value of $(\Delta P_s D/4L)$, i.e. the wall shear stress, as measured from the experiments is of the order $[O(10Pa)]$, similar to the yield stress of Laponite dispersions of comparable concentration and ionic strength^{37,38}. This implies that the material does not shear anywhere in radial direction and moves as a plug, viz. $\lambda \rightarrow 1$. This is clearly observed through flow visualization (see section IV in supplementary information and the accompanying movie file). The material yielding is then the primary reason for slip in present system which is consistent with previous reports¹². Based on these arguments, we consider slip as the predominant behavior which, thereby, leads to simplification of eq. (??) as

$$Q = \frac{\pi}{16} \frac{\Delta P_s}{L} \frac{D^2 \delta^2}{\mu} \quad (2)$$

In this equation, all quantities except δ , are either known, measured or can be estimated. We infer the behavior of δ based on our experiments. Using a linear dependence i.e $\delta \propto Q$ in Eq. 2, we observe that the experimentally obtained inverse relation between ΔP_s and Q is recovered. We reiterate that the linear dependence of δ on Q is invoked to rationalize the data and is not based on any reasoning from the literature. We do note, however, that experiments by Zhu and Granick³⁹ for Newtonian liquids do show that slip length increases with shear rate. Further, neither can the dependence of slip length on system size be obtained from the literature^{2,4,7}. We, thus, consider $\delta \propto Q/f(D)$, where the exact functional dependence on tube diameter is obtained from a fit to the experimental data. Finally, the extensive literature on the effect of ionic strength on Laponite aging indicates that the dependence on salt concentration is highly nonlinear^{23,25,40}. Again out of convenience we invoke a non-linear relation where the viscosity varies with the square of salt concentration,

i.e. $\mu \propto c_s^2$. Using these assumptions, Eq. 2 can be expressed as

$$\frac{\Delta P_s}{L} \propto \frac{c_s^2}{QD^2} [f(D)]^2 \quad (3)$$

The experimental results for all flow rates, tube diameters and salt concentrations studied are shown in fig. 5 (main panel) following Eq. 3. We adjust $f(D)$ so as to collapse the data on a universal curve by shifting individual data sets. We observe that $[f(D)]^2$ shows a power-law dependence on tube diameter (D) with an exponent 1.36 as shown in fig 5(inset). Collapse of data from experiments carried over a wide range of parameters, on a master curve is remarkable given the complexity of microstructure formation in thixotropic Laponite suspensions. From a fit to the data, we obtain the relation $(\Delta P_s/L) \propto c_s^2 Q^{-1} D^{-0.64}$. Further, our data suggests an empirical correlation for the slip length, given as $\delta \propto Q/D^{0.68}$. Though not identical to our experimental system, we note that the slip length has been theoretically shown to scale as D^{-1} for the flow of water through nanopores⁴.

IV. CONCLUSIONS

In summary, we have investigated the slip behavior for pressure driven flow of a thixotropic material through a cylindrical tube. While the Laponite suspension is thixotropic, we obtain steady state flow behavior over a range of experimental conditions. The steady state is envisaged as a balance between the inherent structure formation of Laponite and possible breakage due to flow. The steady state is represented by near time independent (or saturated) pressure values measured during the flow of suspension through the tube.

Remarkably, the saturated pressure drop shows an inverse relation with the flow rate, in contrast to our expectation based on the Poiseuille relation. These observations can be rationalised by invoking slip of Laponite suspensions at the tube walls. We show that the observed experimental results can be accounted for if a linear dependence is assumed between the slip length and flow rate and the material can be described using Bingham constitutive equation. The observed scaling behavior indicate that the slip length varies linearly with the flow rate and inversely with tube diameter.

It is to be, however, noted that the scaling behavior is obtained purely based on a fit to the data. The assumed variations of the key variables cannot be obtained from the literature and their deduction through independent measurements is not within the scope of this work. The reasonably good scaling behavior suggests that these adhoc assumptions are not without merit. The remarkably simple dependence of the flow behavior of a complex thixotropic material should pave the way for a more involved theoretical treatment of flowing thixotropic materials.

SUPPLEMENTARY MATERIAL

Details about the design and characterisation of various flow accessories used in experiments and flow visualisation methodology are provided as supplementary material for ready reference.

ACKNOWLEDGMENTS

AVO gratefully acknowledges the financial support from Science & Engineering Research Board, India (Grant No. SB/S3/CE/017/2015).

DATA AVAILABILITY

The data that support the findings of this study are available from the corresponding author upon reasonable request.

- ¹E. Schnell, “Slippage of water over nonwetable surfaces,” *J. Appl. Phys.* **27**, 1149 (1956).
- ²K. Watanabe and Y. U. nd H. Udagawa, “Drag reduction of newtonian fluid in a circular pipe with a highly water-repellent wall,” *J. Fluid Mech.* **381**, 225–238 (1999).
- ³D. C. Tretheway and C. D. Meinhart, “Apparent fluid slip at hydrophobic microchannel walls,” *Phys. Fluids* **14**, L9 (2002).
- ⁴L. Li, Y. Su, H. Wang, G. Sheng, and W. Wang, “A new slip length model for enhanced water flow coupling molecular interaction, pore dimension, wall roughness and temperature,” *Adv. Polymer Technol.* **2019**, 6424012 (2019).
- ⁵N. V. Churaev, V. D. Sobolev, and A. N. Somov, “Slippage of liquids over lyophobic solid surfaces,” *J. Coll. Int. Sci.* **97**, 574 (1984).
- ⁶S. K. Aghdam and P. Ricco, “Laminar and turbulent flows over hydrophobic surfaces with shear-dependent slip length,” *Phys. Fluids* **28**, 035109 (2016).
- ⁷J. T. Cheng and N. Giordano, “Fluid flow through nanometer-scale channels,” *Phys. Rev. E* **65**, 031206 (2002).
- ⁸E. Lauga and H. A. Stone, “Effective slip in pressure-driven stokes flow,” *J. Fluid Mech.* **489**, 55–77 (2003).
- ⁹D. K. Kalyon, “Apparent slip and viscoplasticity of concentrated suspensions,” *J. Rheol.* **49**, 621 (2005).
- ¹⁰D. M. Kalyon and M. Malik, “Axial laminar flow of viscoplastic fluids in a concentric annulus subject to wall slip,” *Rheol. Acta* **51**, 805 (2012).
- ¹¹J. F. Ortega-Avila, J. Pérez-González, B. M. Marín-Santibáñez, F. Rodríguez-González, S. Aktas, M. Malik, and D. M. Kalyon, “Axial annular flow of a viscoplastic microgel with wall slip,” *J. Rheol.* **60**, 503 (2016).
- ¹²A. Poumaere, M. Moyers-González, C. Castelain, and T. Burghelea, “Unsteady laminar flows of a carboxypol gel in the presence of wall slip,” *J. non-Newt. Fluid Mech.* **205**, 28 (2014).
- ¹³A. S. Haase, J. A. Wood, L. M. J. Sprakel, and R. G. H. Lammertink, “Inelastic non-newtonian flow over heterogeneously slippery surfaces,” *Phys. Rev. E* **95**, 023105 (2017).
- ¹⁴A. Aiyejina, D. P. Chakrabarti, A. Pilgrim, and M. K. S. Sastry, “Wax formation in oil pipelines: A critical review,” *Int. J. Multi. Flow* **37**, 671–694 (2011).
- ¹⁵A. M. van Beerke, J. van Marle, A. K. Groen, and M. J. Bruno, “Mechanisms of biliary stent clogging,” *Endoscopy* **37**, 729–734 (2005).
- ¹⁶G. Donelli, E. Guaglianone, R. D. Rosa, F. Fiocca, and A. Basoli, “Plastic biliary stent occlusion: Factors involved and possible preventiva approaches,” *Clinical Med. Res.* **5**, 53–60 (2007).
- ¹⁷S. Jamali, G. H. McKinley, and R. C. Armstrong, “Microstructural rearrangements and their rheological implications in a model thixotropic elastoviscoplastic fluid,” *Phys. Rev. Lett.* **118**, 048003 (2017).
- ¹⁸J. P. Cunha, P. R. de Souza Mendes, and I. R. Siqueira, “Pressure-driven flows of a thixotropic viscoplastic material: Performance of a novel fluidity-based constitutive model,” *Phys. Fluids* **32**, 123104 (2020).
- ¹⁹D. Bonn, H. Kellay, H. Tanaka, G. Wegdam, and J. Meunier, “Laponite: What is the difference between a glass and a gel?” *Langmuir* **15**, 7534–7536 (1999).
- ²⁰A. Knaebel, M. Bellour, J. P. Munch, V. Viasnoff, F. Lequeux, and J. L. Harden, “Aging behavior of laponite clay particle suspensions,” *Eur. Phys. Lett.* **52**, 73 (2000).
- ²¹D. Bonn, S. Tanase, B. Abou, H. Tanaka, and J. Meunier, “Laponite: Aging and shear rejuvenation of a colloidal glass,” *Phys. Rev. Lett.* **89**, 015701 (2002).
- ²²B. Ruzicka, L. Zulian, E. Zaccarelli, R. Angelini, M. Sztucki, A. Moussaid, and G. Ruocco, “Competing interactions in arrested states of colloidal clays,” *Phys. Rev. Lett.* **104**, 085701 (2010).
- ²³B. Ruzicka and E. Zaccarelli, “A fresh look at the laponite phase diagram,” *Soft Mat.* **7**, 1268–1286 (2011).
- ²⁴S. Jataw and Y. M. Joshi, “Rheological signatures of gelation and effect of shear melting on aging colloidal suspension,” *J. Rheol.* **58**, 1535–1554 (2014).
- ²⁵K. Suman and Y. M. Joshi, “Microstructure and soft glassy dynamics of aqueous laponite dispersion,” *Langmuir* **34**, 13079–13103 (2018).
- ²⁶P. Levitz, E. Lecolier, A. Mourchid, A. Delville, and S. Lyonnard, “Liquid-solid transition of laponite suspensions at very low ionic strength: Long-range electrostatic stabilisation of anisotropic colloids,” *Eur. Phys. Lett.* **49**, 672 (2000).
- ²⁷D. Bonn, H. Tanaka, G. Wegdam, H. Kellay, and J. Meunier, “Aging of a colloidal “wigner” glass,” *Eur. Phys. Lett.* **45**, 52 (1998).
- ²⁸H. Tanaka, J. Meunier, and D. Bonn, “Nonergodic states of charged colloidal suspensions: Repulsive and attractive glasses and gels,” *Phys. Rev. E.* **69**, 031404 (2004).
- ²⁹A. Mourchid, A. Delville, J. Lambard, E. Lecolier, and P. Levitz, “Phase diagram of colloidal dispersions of anisotropic charged particles: equilibrium properties, structure, and rheology of laponite suspensions,” *Langmuir* **11**, 1942–1950 (1995).
- ³⁰F. Pignon, J. M. Piau, and A. Magnin, “Structure and pertinent length scale of a discotic clay gel,” *Phys. Rev. Lett.* **76**, 4857 (1996).

- ³¹F. Pignon, A. Magnin, and J. M. Piau, “Butterfly light scattering pattern and rheology of a sheared thixotropic clay gel,” *Phys. Rev. Lett.* **79**, 4689 (1997).
- ³²F. Pignon, A. Magnin, J. M. Piau, P. L. B. Cabane, and O. Diat, “Yield stress thixotropic clay suspension: Investigations of structure by light, neutron, and x-ray scattering,” *Phys. Rev. E.* **56**, 3281 (1997).
- ³³M. Kroon, G. Wegdam, and R. Sprik, “Dynamic light scattering studies on the sol-gel transition of a suspension of anisotropic colloidal particles,” *Phys. Rev. E.* **54**, 6541 (1996).
- ³⁴M. Kroon, W. Vos, and G. Wegdam, “Structure and formation of a gel of colloidal disks,” *Phys. Rev. E.* **57**, 1962 (1998).
- ³⁵R. Avery and J. Ramsay, “Colloidal properties of synthetic hectorite clay dispersions: Ii. light and small angle neutron scattering,” *J. Colloid Interface Sci.* **109**, 448–454 (1986).
- ³⁶T. Nicolai and S. Cocard, “Light scattering study of the dispersion of laponite,” *Langmuir* **16**, 8189–8193 (2000).
- ³⁷P.-I. Au and Y.-K. Leong, “Surface chemistry and rheology of laponite dispersions - zeta potential, yield stress, ageing, fractal dimension and pyrophosphate,” *Appl. Clay Sci.* **107**, 36–45 (2015).
- ³⁸Y. Lin, H. Zhu, W. Wang, J. Chen, N. Phan-Thien, and D. Pan, “Rheological behavior for laponite and bentonite suspensions in shear flow,” *AIP Adv.* **9**, 125233 (2019).
- ³⁹Y. Zhu and S. Granick, “Rate-dependent slip of newtonian liquid at smooth surfaces,” *Phys. Rev. Lett.* **87**, 096105 (2001).
- ⁴⁰Y. M. Joshi and G. Petekidis, “Yield stress fluids and ageing,” *Rheol. Acta* **57**, 521–549 (2018).